Multi Objective Optimisation of the Dynamic Behaviour in Robotics

A Olaru[1], T Dobrescu[2], S Olaru[3], N Mihai[4] and N Smidova[5]

[1]Laboratory of Robots Dynamic Behaviour, *Politehnica University of Bucharest,* 313 Splaiul Independentei Street, 060042 Bucharest, Romania
[2]Head of Robotics and Production Systems Dpt., *Politehnica University of Bucharest*
[3]Aviation Laboratory, *Metra National Agency*, Bucharest, Romania
[4]Research Laboratory, *Techno Accord Company,* Leuval, Canada
[5]Physics Laboratory, *Technical University*, Kosice, Slovakia

[1]E-mail: aolaru_51@ymail.com

Abstract. Multi objectives optimisation in the dynamic behaviour of robots is one of the most difficult problem to be solved. In the paper will be shown the complex matrix form of the active forces and moments in the robot's joints, the mathematical models for the inertial tensors for different form of the robot's body and the proper algorithm to establish the best case between some studied cases when were changed: the movements- simultaneously, successive or combination of them; the dimensions of the bodies; the constant velocity of each trapezoidal characteristics; the acceleration and deceleration time. The mathematical matrix form of the active forces and moments equations were transposed in to the virtual LabVIEW instrumentation with the goals to obtain some characteristics of the active forces and moments variation vs. time in each joints of the robot, in the cases when were changed some functional or constructive parameters. In controlling the movements of the end-effector and joints of a manipulator in the workspace, an important problem is to identify the joints' best relative displacements to assure extreme precisions for the end-effector movements. Applications where multiple manipulators with a common controller to be controlled in 3D space are more challenging compared to single robot control since the movements of the end-effectors of all robots must be determined using complex forward (FK) and inverse kinematics (IK).The presented method is a multi-objective technique with the employed Virtual LabVIEW Instrumentations (VI) for the assisted research of the robot joint's moments that could be generalized to other robots tracking for any conventional and unconventional space curves. By using proper optimization algorithm was choose the best solution between all these studied cases. The applied method, the algorithm and the proper virtual instrumentation solve one small part of the complex problems of the optimisation of the dynamic behaviour in robotics.

1. Introduction

A multi-robot system is a collection of robots, collaborating together to fulfill the global goal. Every robot is a physical agent equipped with processors and sensors to be able to perform independent operation and individual autonomous behaviors. Numerous applications of multi-robot systems can be found, such as environmental surveillance and monitoring [1-12](Chaimowicz et al. 2005), search and rescue (Bhattacharya et al. 2013b), risky material removal, and so on. The environment is partitioned into regions and each robot of the team should be responsible for covering the events happening inside its assigned region. To measure the performance of any specific solution, a deployment function represents the quality of the robots distribution over the field. Such a function might be defined based on the distance of robots to the points in the environment, which must be minimized. Minimizing motion time can significantly shorten cycle time, increase the productivity, improve machine utilization, and thus make automation affordable in applications for which throughput and cost effectiveness is of major concern. In industrial application, a robotic manipulator performs a repetitive sequence of movements. A *manipulability measure* was proposed [13-22] (Yoshikawa, 1985) and a modification to Yoshikawa's manipulability measure was proposed (Tsai, 1986)[15,16] which also accounted for proximity to joint limits. (Nelson & Donath, 1990) [12] developed a gradient function of manipulability in Cartesian space based on explicit determination of manipulability function and the gradient of the manipulability function in joint space. Then they used a modified method of the steepest descent optimization procedure (Luenberger, 1969) [10] as the basis for an algorithm that automatically locates an assembly task away from singularities within manipulator's workspace. The IRC5 robot controller uses powerful, configurable software and has a unique dynamic model-based control system which provides self-optimizing motion (Vukobratovic, 2002)[17]. The entire robot, robot tool, targets, path, and coordinate systems can be defined and specified in RobotStudio. The simulation of a robot system in RobotStudio employs the ABB Virtual Controller, the real robot program, and the configuration file that are identical to those used on the factory floor. In the field of rigid robotics could be uses dedicated products like WorkspaceLt [38], RoboticSimulation [39], NI-Robotics [40] RoboNaut [41] or SimRobot [42] or general purpose open-source software like Gazebo [36]. The cited tools rely on off-the-shelves simulation kernels such as Open Dynamics Engine [43], Bullet Physics [44], NVidia PhysX [45] or DART [46].

In the paper [22-46] authors by using the special software RoboAnalyzer, Robotech, V-Rep, RoKiSim, Ros, WorkspaceLt, RoboticSimulation, NI-Robotics, RoboNaut, SimRobot, Gazepo show some characteristics and solve direct and inverse kinematics problem and also the direct and inverse dynamic problem, but without show the mathematical matrix model and how could be influenced the force and moments variation by different velocity characteristics or to obtain or choose the minimum variation of the forces and moments between some studied cases.

This paper show some virtual instrumentation for the assisted research of the robot positions, velocities, accelerations, forces and moments in some different cases when were changed some parameters of the velocity characteristics and how could be find the best solution between these cases, using the multi- objective functions, one proper algorithm, Extenics and Neutrosophic theory [20,21].

2. Experimental setup

The experimental setup content one didactical arm type robot with 4 DOF, with DC motors with encoders, with Geko drive GK330, acquisition board and LabVIEW software. This setup was used to validate some of the matrix model for the positions and velocities and some *VI*-s for controlling the space trajectory. We used one complex program for the 3D space trajectory to show and verify some of the theoretical space trajectory. The mathematical model was written by using the configuration of this robot and also all inertial moments and space tensors J_{gi} were calculated using the dimension of this robot's bodies. The theoretical active moments determined by using the model and *VI*-s were verified.

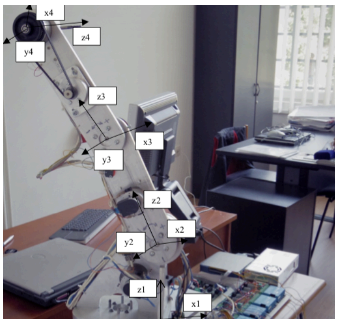

Figure 1. The didactical art type robot used in the research

3. Mathematical model of the dynamic behaviour

Mathematical model is complex and contents in the matrix form the Forward Kinematics (FK), Inverse Kinematics (IK), Direct Dynamics (DD) and Inverse Dynamics (ID). The kinematics equations were written in 3x3 and 6x6 form and the dynamic equations were written in (DOFx3)x(DOFx3). In the experimental cases what were analysed, these equations were written in 12x12 form. Without assisted analyse with LabVIEW virtual instrumentation it would not have been possible to determine the forces and moments variations in all robot's joints and to calculate the Multi Objective Function (*MOF*) establishing finally what it is the best dynamic solution between the all studied cases.

The recurrent 3x3 matrix equation in positions analyse is:

$$\left(r_i^0\right) = \left(r_{i-1}^0\right) + \left[D_{i-1}^0\right]\left(r_i^{i-1}\right) \tag{1}$$

The recurrent 6x6 matrix equations in the velocities analyse are:

$$\begin{pmatrix} \left(\omega_{i,0}^i\right) \\ \left(v_{i,0}^i\right) \end{pmatrix} = \left[T_{i-1}^i\right] \begin{pmatrix} \left(\omega_{i-1,0}^{i-1}\right) \\ \left(v_{i-1,0}^{i-1}\right) \end{pmatrix} + \begin{pmatrix} \left(\omega_{i,i-1}^i\right) \\ \left(v_{i-1,i}^i\right) \end{pmatrix} \tag{2}$$

$$\begin{pmatrix}(\omega_{i,0}^{0})\\(v_{i,0}^{0})\end{pmatrix}=\begin{bmatrix}[D_i^0] & [0]\\ [0] & [D_i^0]\end{bmatrix}\begin{pmatrix}(\omega_{i,0}^{i})\\(v_{i,0}^{i})\end{pmatrix} \tag{3}$$

The recurrent 6x6 matrix equations in the acceleration analyse are:

$$\begin{pmatrix}(\varepsilon_{i,0}^{i})\\(a_{i,0}^{i})\end{pmatrix}=\left[T_{i-1}^{i}\right]\begin{pmatrix}(\varepsilon_{i-1,0}^{i-1})\\(a_{i-1,0}^{i-1})\end{pmatrix}+(S''(i)) \tag{4}$$

$$(S''(i))=\begin{pmatrix}(\varepsilon_{i,i-1}^{i})+(\widehat{\omega}_{i-1,0}^{i})(\omega_{i,i-1}^{i})\\ (a_{i,i-1}^{i})+(\widehat{\omega}_{i-1,0}^{i})^2(r_{i,i-1}^{i})+2(\widehat{\omega}_{i-1,0}^{i})(v_{i,i-1}^{i})\end{pmatrix} \tag{5}$$

$$\begin{pmatrix}(\varepsilon_{i,0}^{0})\\(a_{i,0}^{0})\end{pmatrix}=\begin{bmatrix}[D_i^0] & [0]\\ [0] & [D_i^0]\end{bmatrix}\begin{pmatrix}(\varepsilon_{i,0}^{i})\\(a_{i,0}^{i})\end{pmatrix} \tag{6}$$

$$(a_{gi,0})^0=\begin{pmatrix}[D_1^0](a_{g1,0}^{1})\\ [D_2^0](a_{g2,0}^{2})\\ [D_3^0](a_{g3,0}^{3})\\ [D_4^0](a_{g4,0}^{4})\\ \ldots\end{pmatrix} \tag{7}$$

$$\left[T_{i-1}^{i}\right]=\begin{bmatrix}\left[D_{i-1}^{i}\right] & 0\\ -\left[D_{i-1}^{i}\right]\left[\widehat{r}_{i}^{i-1}\right] & \left[D_{i-1}^{i}\right]\end{bmatrix} \tag{8}$$

The forces 12x12 matrix equations, mass and transfer matrices are:

$$(P)^0=[z_u]\{(F)^0\pm[m_u](a_{gi,0})^0\} \tag{9}$$

$$[z_u]=\begin{vmatrix}\cdots & \cdots & \cdots\\ \cdots & z_{i,j} & \cdots\\ \cdots & \cdots & \cdots\end{vmatrix}\; z_{i,j}=\begin{pmatrix}-1-oposite\ of\ the\ graph\ sense\\ 1-same\ sens\ of\ the\ graph\\ 0-do't\ touch\ the\ graph\end{pmatrix} \tag{10}$$

$$(F^0)=\begin{pmatrix}[D_1^0](F_1^1)\\ [D_2^0](F_2^2)\\ [D_3^0](F_3^3)\\ [D_4^0](F_4^4)\\ \ldots\ldots\end{pmatrix} \tag{11}$$

$$[D_4^0]=[D_1^0][D_2^1][D_3^2][D_4^3]$$

$$[D_i^j]=\begin{bmatrix}1 & 0 & 0\\ 0 & c & -s\\ 0 & s & c\end{bmatrix} or \begin{bmatrix}c & 0 & -s\\ 0 & 1 & 0\\ s & 0 & c\end{bmatrix} or \begin{bmatrix}c & -s & 0\\ s & c & 0\\ 0 & 0 & 1\end{bmatrix} \tag{12}$$

$$[F_1^1]=\begin{bmatrix}0\\0\\-m_1g\end{bmatrix}$$

$$[m_u]=\begin{bmatrix}m_1\begin{bmatrix}1&0&0\\0&1&0\\0&0&1\end{bmatrix} & 0 & 0\ldots\\ 0 & m_2\begin{bmatrix}1&0&0\\0&1&0\\0&0&1\end{bmatrix} & 0\ldots\\ 0 & 0 & \ldots\end{bmatrix} \tag{13}$$

The 12x12 matrix equations of the moments, inertial moments variations and anti-symmetrical force's arms are the following form:

$$(Q) = [z_u][(M^0) - (\dot{K}_{gi}^0) + [\widehat{B_i^0}] \times (P_i^0)] \tag{14}$$

$$(M^0) = \begin{pmatrix} D_1^0 M_1^1 \\ D_2^0 M_2^2 \\ D_3^0 M_3^3 \\ D_4^0 M_4^4 \end{pmatrix} \tag{15}$$

$$(\dot{K}_{gi}^0) = \begin{pmatrix} [D_1^0](\dot{K}_{g1}^1) \\ [D_2^0](\dot{K}_{g2}^2) \\ [D_3^0](\dot{K}_{g3}^3) \\ [D_4^0](\dot{K}_{g4}^4) \end{pmatrix} \tag{16}$$

$$[\dot{K}_{gi}^i] = [J_{gi}^i](\varepsilon(i)) + [\widehat{\omega}_{i-1,0}^i][J_{gi}^i](\omega(i)) \tag{17}$$

$$[J_{gi}^i] = \begin{bmatrix} J_{xx} & -J_{xy} & -J_{xz} \\ -J_{yx} & J_{yy} & -J_{yz} \\ -J_{zx} & -J_{zy} & J_{zz} \end{bmatrix} \tag{18}$$

Inertial tensor for the robot with parallelepiped form of the bodies and with Cartesian system on the middle of the base plane is: (19)

$$[J_{gi}^i] = \begin{bmatrix} \frac{m(B^2+C^2)}{3} + m(b^2+c^2) + m(Bb+Cc) & -(\frac{mAB}{4} + \frac{mAb}{2} + \frac{mBc}{2} + mab) & -(\frac{mAC}{4} + \frac{mAc}{2} + \frac{mCc}{2} + mac) \\ -(\frac{mAB}{4} + \frac{mAb}{2} + \frac{mBc}{2} + mab) & \frac{m(A^2+C^2)}{3} + m(c^2+a^2) + m(Cc+Aa) & -(\frac{mBC}{4} + \frac{mBc}{2} + \frac{mCb}{2} + mbc) \\ -(\frac{mAC}{4} + \frac{mAc}{2} + \frac{mCc}{2} + mac) & -(\frac{mBC}{4} + \frac{mBc}{2} + \frac{mCb}{2} + mbc) & \frac{m(B^2+A^2)}{3} + m(a^2+b^2) + m(Aa+Bb) \end{bmatrix}$$

$$\hat{B}^0 = \begin{bmatrix} & & \cdots & & \\ \vdots & \ddots \ \cdots & \hat{b}_{i,k}^0 G_k^0 & \cdots & \vdots \\ & & \cdots & & \end{bmatrix} \tag{20}$$

$$b_{i,k}^0 = r_k^0 - r_{gi}^0 \tag{21}$$

$$\hat{b}_{i,k}^0 = \begin{bmatrix} 0 & -b_{i,k,z}^0 & b_{i,k,y}^0 \\ b_{i,k,z}^0 & 0 & -b_{i,k,x}^0 \\ -b_{i,ky}^0 & b_{i,k,x}^0 & 0 \end{bmatrix} \tag{22}$$

Where: $(r^0{}_i)$ is the column matrix vector for absolute position i joint versus the base Cartesian system; $(r^0{}_{i-1})$- column matrix vector for absolute position i-1 joint; $[D^0{}_{i-1}]$- quadratic matrix for transfer vector from i-1 to base system; $\begin{pmatrix} (\omega_{i,0}^0) \\ (v_{i,0}^0) \end{pmatrix}$ – is the dual matrix vector of the absolute angular and linear velocity of the i joint versus the Cartesian base system; $\begin{pmatrix} (\omega_{i,0}^i) \\ (v_{i,0}^i) \end{pmatrix}$ - is the dual matrix vector of the absolute angular and linear velocity of the i joint versus the i Cartesian system; $\begin{pmatrix} (\varepsilon_{i,0}^i) \\ (a_{i,0}^i) \end{pmatrix}$-is the dual matrix vector of the absolute acceleration of the i joint versus the i Cartesian system; $\begin{pmatrix} (\varepsilon_{i,0}^0) \\ (a_{i,0}^0) \end{pmatrix}$- the dual matrix vector of the absolute acceleration of the i joint versus the base Cartesian system; $\begin{pmatrix} (\varepsilon_{i-1,0}^{i-1}) \\ (a_{i-1,0}^{i-1}) \end{pmatrix}$- the dual matrix vector of the absolute acceleration of the i-1 joint versus the i-1 Cartesian system; $\left[T_{i-1}^{i}\right]$-the quadratic 6x6 transfer matrix from the i-1 to i system; $(S''(i))$- the dual matrix vector of the relative joint's acceleration between i and i-1 joint versus i Cartesian system; $(\varepsilon_{i,i-1}^{i})$- the column matrix vector of the relative angular acceleration between i and i-1 systems versus i Cartesian system; $(\widehat{\omega}_{i-1,0}^{i})$- antisimetrical absolute vector of the angular velocity of the i-1 joint versus i Cartesian system; $(\omega_{i,i-1}^{i})$- velocity angular relative column matrix vector between i and i-1 joints; $\left(a_{i,i-1}^{i}\right)$ – linear relative acceleration column matrix form between i and i-1 joint versus i Cartesian system; $(\widehat{\omega}_{i-1,0}^{i})^2(r_{i,i-1}^{i})$- column matrix centrifuge relative acceleration between i and i-1 joints versus i Cartesian system; $2(\widehat{\omega}_{i-1,0}^{i})(v_{i,i-1}^{i})$- column matrix form of the Coriolis relative acceleration between i and i-1 joints versus i Cartesian system; i- the current robot's joint and have the 1-5 values; (P^0)- is the active force matrix reduced to the base; $[z_u]$- unitary joints-bodies matrix; (F^0)- resistive force matrix reduced to the base; (F_i^i)- resistive force matrix reduced to the proper cartesian system; $[D_i^j]$- transfer matrix from the i Cartesian system to j Cartesian system; $[m_u]$- mass matrix, or where m_i was multiply by unitary matrix for the space;(Q)- column matrix of the active moments in a joints; (M^0)- column matrix of the resistant moments in a joints; $[\hat{B}_i^0]$- antisymmetric force's arm matrix; (P_i^0)- column matrix for active forces; $(\dot{K}_{gi}^{0})$- column matrix of the variation of the inertial moment reduced to the base Cartesian system; $(\dot{K}_{gi}^{i})$- column matrix of the variation of the inertial moment reduced to the i Cartesian system; A,B,C- the dimension of the robot's body of the *ox*, *oy* and *oz* axes; *a, b, c* – distance between the *OX, OY, OZ* axes of the Cartesian base system and the *ox, oy, oz* axes of the Cartesian system of the robot's body; $[G_k^0]$ – bodies- joints matrix of the robot determined by the associated graph; $[J_{gi}^{i}]$- matrix of the inertial tensor reduced to the i proper Cartesian system.

4. Instrumentation LabVIEW used in the assisted research

The front panel of the LabVIEW VI-s used in the assisted research is shown in figures 2-12. The programme have one part of the input data fig.2 and one part with the results fig.3 (the characteristics of all active moments in the robot's joints vs. time, determined for some different cases of the movements. These cases were: 0-0-0-0 all movements are simultaneously with the same velocities and time of cycle; 0-3-3-0 the first and the last joint's movements are simultaneously and second and third are successive after 3 seconds. In some of cases were changed also the velocity, or the movements were successively after the acceleration time of each of them. Other figs. contents the icons of all sub*VI*-s.

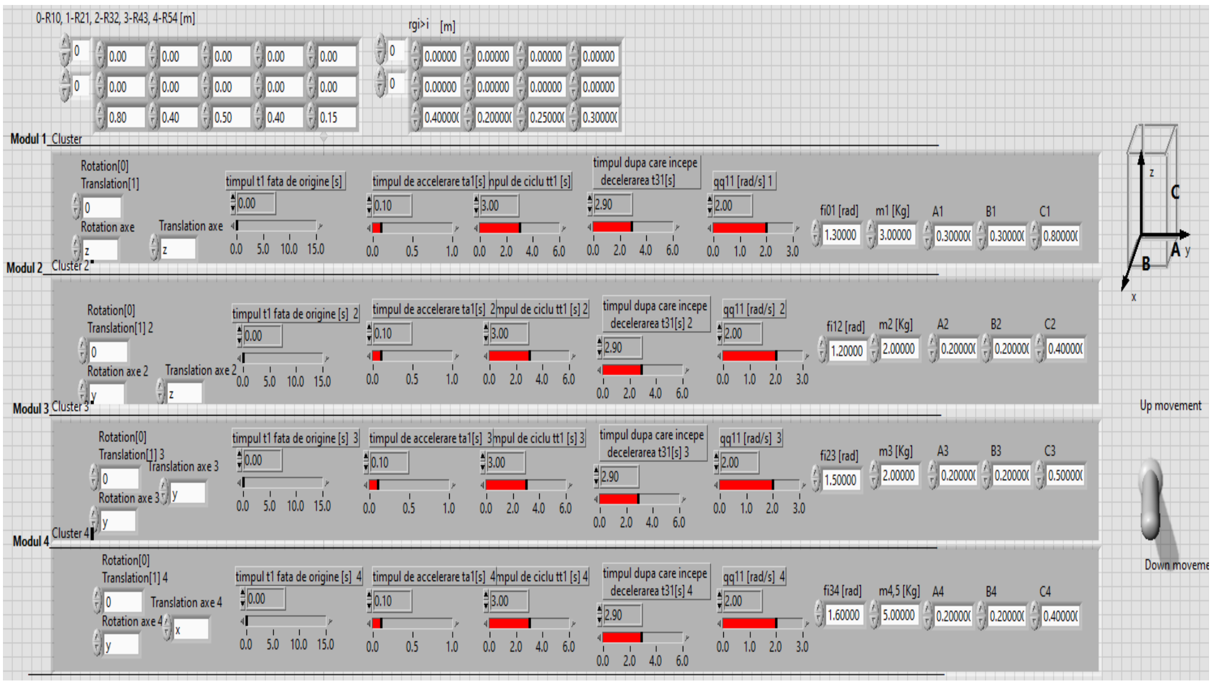

Figure 2 Front panel of the LabVIEW VI-s for the assisted research of the active moments in the robot's joints

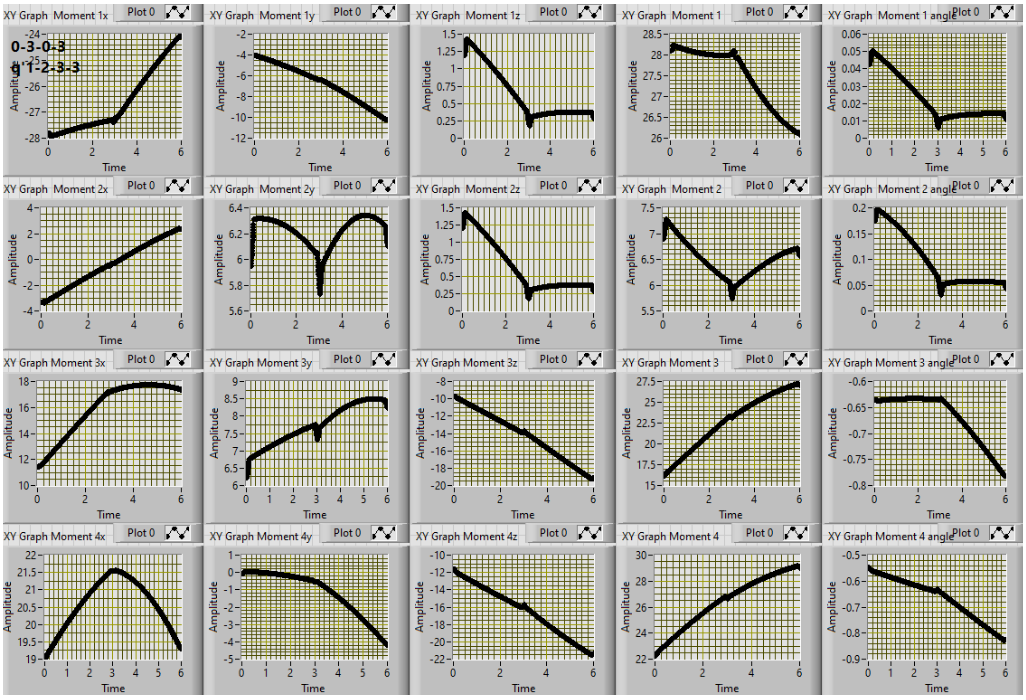

Figure 3 Front panel of the LabVIEW VI-s with the active moments variation vs. time

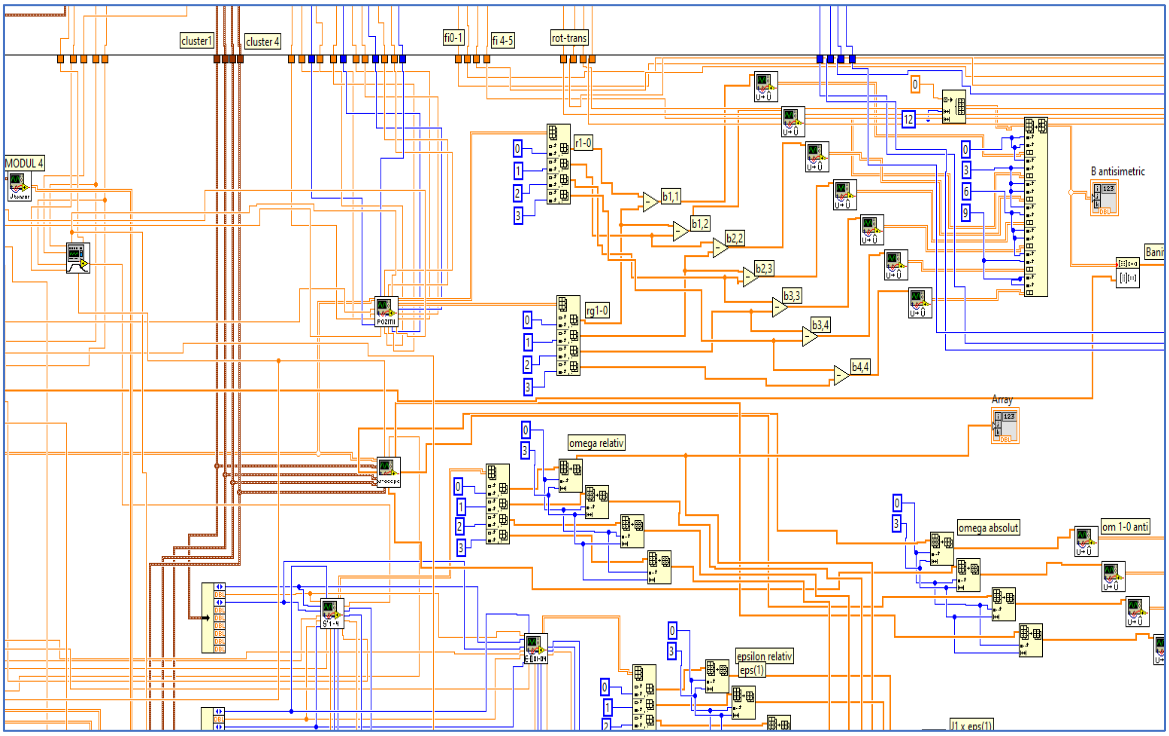

Figure 4 Part of the block diagram of the used *VI*-s

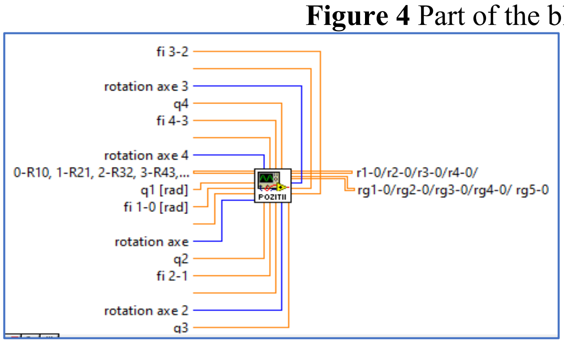

Figure 5 Icon of the position analyse

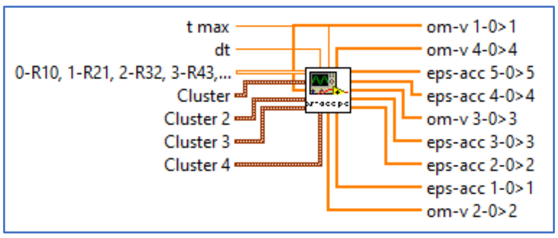

Figure 6 Icon of the acceleration analyse

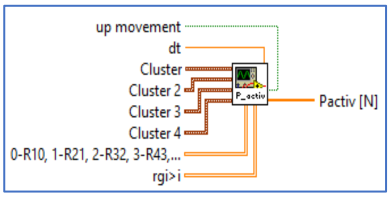

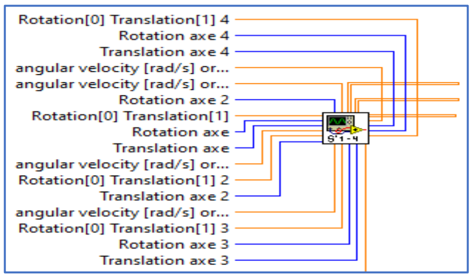

Figure 7 Icon of the active forces **Figure 8** Inertial tensor *VI*-s **Figure 9** Icon of velocities analyse

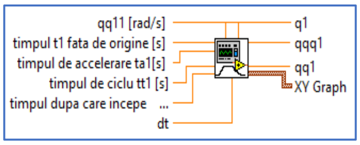

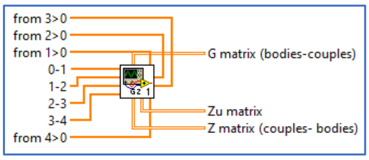

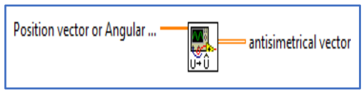

Figure 10 Icon of trapezoidal velocity **Figure 11** Icon of the *Z* matrix **Figure 12** Icon antisymmetric

5. Multi objective analyse

One way to optimize the active robot joint's moments were determined by using one multi objective optimization function. This multi objective function trying to choose the case between all these studied cases that have the minimum variation of all joint's moments. The used algorithm contents the following steps: (i) determine the variation of the moments vs. time by using the characteristics for different cases concerning some different velocity trapezoidal characteristics, some different dimensions of the bodies, some different established constructive and functional parameters of the robot that could be studied; (ii) determine some moments characteristics by change some of the constructive or functional parameters, or type of velocity characteristics; (iii) determine the table with the maximal range of all these moments; (iv) impose for each of moments, one maximal pounder (if all moments are the same impact to the global dynamic behaviour of the robot- the values of all pounders will be the same- in these studied cases, the each pounder p_i was 100); (v) calculate for each moment and cases, the pounder values by using the proportion between the minimum value of each moment variation and the current variation from minimum to maximum moment and multiply with the maximum pounder values (using also the Neutrosophic theory of Smarandache and Extenics theory of Cai Wen)[20,21]; (vi) calculate separately for up and down movements of the robot's arm and determine the case what the sum of these total pounders have maximal value that determine the minimum values of the moments variation in each robot's joint.

Mathematic we can write this multi objective function (*MOF*) like in relation (23):

$$\boldsymbol{MOF(t_i, tt_i, t_{ai}, t_{di}, l_i, \varphi_i)} = \tag{23}$$

$$\mathbf{min}\ (\mathbf{rangeM_{1x,y,z}}) \cap \mathbf{min}\ (\mathbf{range|M|_1} \cap \mathbf{min}\ (\mathbf{range} < \mathbf{M_1}) \cap\ \mathbf{min}\ (\mathbf{rangeM_{2x,y,z}} \cap \mathbf{min}\ (\mathbf{range|M|_2}) \cap \mathbf{min}\ (\mathbf{range} < \mathbf{M_2}) \cap\ \mathbf{min}\ (\mathbf{rangeM_{3x,y,z}} \cap \mathbf{min}\ (\mathbf{range|M|_3}) \cap \mathbf{min}\ (\mathbf{range} < \mathbf{M_3}) \cap \mathbf{min}\ (\mathbf{rangeM_{4x,y,z}}) \cap \mathbf{min}\ (\mathbf{range|M|_4}) \cap \mathbf{min}\ (\mathbf{range} < \mathbf{M_4})$$

where: t_i is the time to origin of time [s]; tt_i- the cycle time [s]; t_{ai}- the acceleration time [s]; t_{di}- the time when begin the deceleration [s]; l_i- the length of each body [m]; φ_i- angle position of each body [rad]; $M_{i,x,y,z}$- active moment in each joints [Nm]; $|\boldsymbol{M_i}|$- module of the active moment in each joints, [Nm]; $< \boldsymbol{M_i}$ - angle in a space of each active moment vector, [rad].

This *MOF* function have 20 conditions to be simultaneously touch, but that will be possible by using Neutrosophic theory [16,17], that mince all these conditions will be touch between T (true) and F (false)= p_i(T)∪p_j(F) where $p_{i,j}$ are the ponders for each criteria and for each cases, otherwise the *MOF* result will be null, because it is impossible that all 20 moments components for each of studied cases to be minimum in the same time.

$$\boldsymbol{MOF} = \mathbf{max}\ \left(\sum_1^{20} \boldsymbol{p_i} \frac{\boldsymbol{M_{i,x,y,z,<,min}}}{\boldsymbol{M_{i,x,y,z,<,crt}}}\right)_{\text{cases}} \tag{24}$$

where: p_i is the maximal pounder for each; $\boldsymbol{M}_{i,x,y,z,<,min}$- the minimum value of each of these moments and angle's moments; $\boldsymbol{M}_{i,x,y,z,<,crt}$- the current value of the moments for each of the studied cases.

The cases that were studied are the following: 0-0-0-0 all movements are simultaneously; 0-3-3-0 the first and four movements are simultaneously and the second and third will simultaneously, but successive after 3s after the first and fourth; 0-3-6-9 all movements are successive; 0-0.1-0.2-0.3 the movements are successive after the acceleration time of each of them; 0-2.9-5.8-8.7 the movements are successive after the constant velocity time from the velocity characteristics; 0-0-0-0 q_i 1-2-3-3 -all movements are simultaneously, but were changed the velocities in all robot's joints.

Some of the results of the simulation mathematical matrix model rel.(1-22) are shown in figs.13-14.

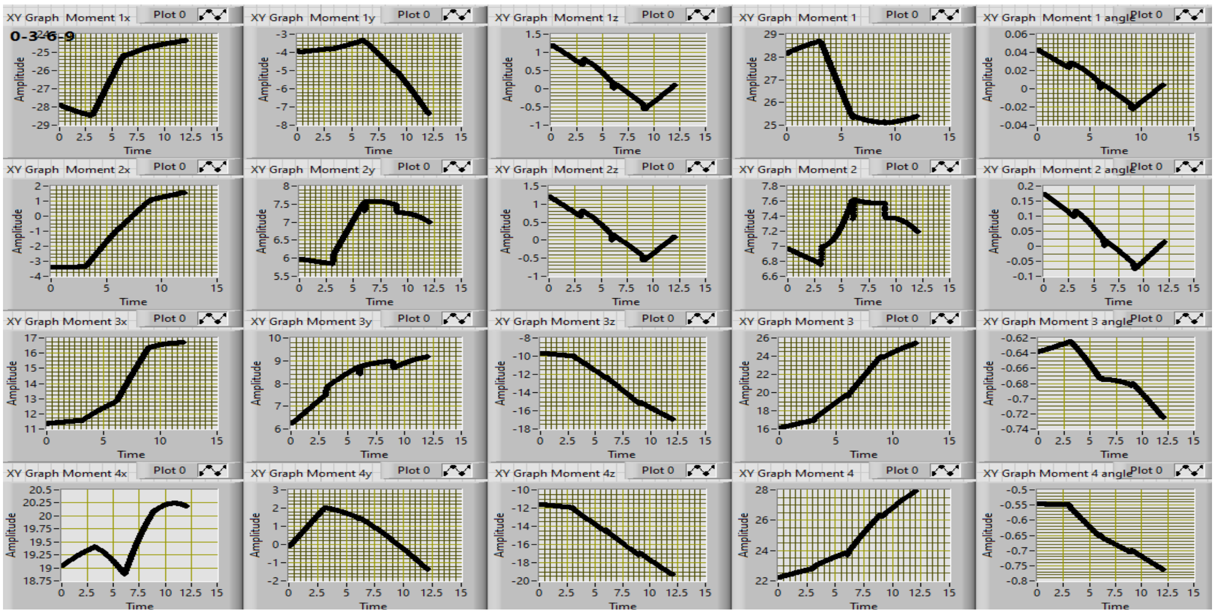

Figure 13 Front panel with the variation of the active moments in a robot's joints- case 0-3-6-9

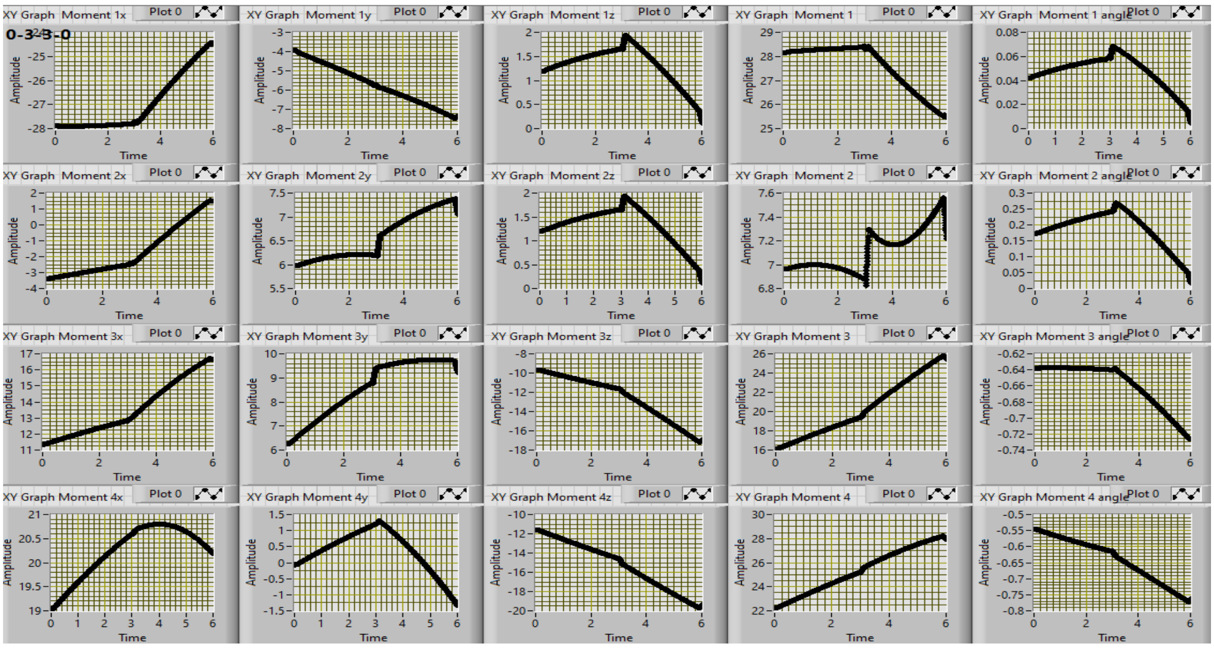

Figure 14 Front panel with the variation of the active moments in a robot's joints- case 0-3-3-0

After were analysed all simulation results were determined the maximal range of all moments and the space angle of them and were calculated the pounders. The results are shown in the table 1 and 2. The best solution was case with simultaneously movements in all joints-case 0-0-0-0. In red colour is the minimum criteria's range and the best solution of the studied cases.

Table 1 The maximal range of the moments variation in all robot's joints

case	M1x	M1y	M1z	M1	<M1	M2x	M2y	M2z	M2	<M2
0-3-6-9	5,00	4,50	1,80	4,00	0,06	4,50	2,20	1,80	0,80	0,47
0-0-0-0	4,00	4,00	1,50	0,90	0,06	5,00	1,50	1,50	0,80	0,20
0-0.1-0.2-0.3	3,80	3,50	1,40	3,00	0,05	5,00	1,50	1,50	0,60	0,20
0-2.9-5.8-8.7	2,50	3,50	1,80	3,50	0,07	5,00	1,30	1,70	0,80	0,28
0-3-3-0	3,50	4,00	2,00	3,30	0,07	5,00	1,50	2,00	0,80	0,28
0-0-3-3	4,00	4,20	1,25	3,00	0,05	5,00	1,80	1,30	0,70	0,20
3-3-0-0	2,50	4,50	1,80	3,00	0,06	5,00	1,50	1,60	1,25	0,25
0-3-0-3	3,50	3,80	1,40	2,80	0,04	5,00	1,50	1,20	1,25	0,16
0-2.9-2.9-0	4,00	4,00	2,00	3,40	0,05	4,50	1,40	2,00	0,70	0,25
2.9-0-0-2.9	3,80	3,80	1,80	3,50	0,06	5,00	1,60	1,70	0,80	0,23
2.9-0-2.9-0	4,00	3,80	1,50	4,50	0,06	5,00	1,90	1,60	1,20	0,23
0-2.9-0-2.9	2,50	3,80	1,25	2,00	0,05	5,00	1,20	1,25	1,25	0,20
0-2.9-0-2.9 q'=1-2-3-3	4,00	7,00	1,25	2,30	0,04	5,70	0,45	1,25	1,50	0,15
0-0-0-0 q'=1-2-3-3	4,00	6,80	1,25	2,30	0,04	5,50	0,50	1,20	1,30	0,14
minimum range	2,50	3,50	1,25	0.9	0.04	4,50	0,45	1,20	0,60	0,14

M3x	M3y	M3z	M3	<M3	M4x	M4y	M4z	M4	<M4
6,00	3,00	7,00	10,00	0,09	1,30	4,00	8,00	7,00	0,23
6,00	3,80	8,00	10,00	0,09	1,30	1,70	8,00	6,00	0,25
5,60	3,90	7,50	9,00	0,08	1,40	1,90	8,00	7,00	0,25
6,00	3,00	7,80	9,50	0,13	0,50	3,50	7,80	6,00	0,25
6,00	3,00	8,00	9,80	0,10	1,70	2,80	9,00	6,00	0,25
6,00	3,30	7,80	9,60	0,08	1,30	3,00	8,30	4,00	0,26
5,00	3,00	8,00	9,80	0,08	2,00	2,00	8,00	6,00	0,25
6,00	3,80	7,80	9,00	0,12	2,30	2,80	8,00	6,00	0,30
5,80	3,80	8,00	9,80	0,08	1,80	2,80	8,50	6,00	0,25
5,00	3,00	7,80	9,00	0,08	1,10	1,70	8,00	7,00	0,24
5,50	3,40	8,00	9,60	0,08	1,20	1,60	8,00	6,00	0,20
5,00	3,50	7,50	9,00	0,12	2,40	2,50	8,00	7,00	0,20
7,00	2,40	10,00	10,50	0,18	2,50	4,50	10,00	7,00	0,25
6,80	2,50	7,80	11,50	0,17	2,50	4,30	10,00	7,00	0,35
5,00	2,40	7,00	9,00	0,08	0,50	1,60	7,80	4,00	0,20

Table 2 The assisted results after was applied the *MOF* (the relations 23 and 24)

case	M1x	M1y	M1z	M1	<M1	M2x	M2y	M2z	M2	<M2
0-3-6-9	50,0000	77,77778	69,44444	22,5	66,66667	100	20,45455	66,66667	75	29,78723
0-0-0-0	62,5000	87,5	83,33333	100	72,72727	90	30	80	75	70
0-0.1-0.2-0.3	65,7895	100	89,28571	30	80	90	30	80	100	70
0-2.9-5.8-8.7	100,0000	100	69,44444	25,71429	57,14286	90	34,61538	70,58824	75	50
0-3-3-0	71,4286	87,5	62,5	27,27273	57,14286	90	30	60	75	50
0-0-3-3	62,5000	83,33333	100	30	80	90	25	92,30769	85,71429	70
3-3-0-0	100,0000	77,77778	69,44444	30	66,66667	90	30	75	48	56
0-3-0-3	71,4286	92,10526	89,28571	32,14286	100	90	30	100	48	87,5
0-2.9-2.9-0	62,5000	87,5	62,5	26,47059	80	100	32,14286	60	85,71429	56
2.9-0-0-2.9	65,7895	92,10526	69,44444	25,71429	66,66667	90	28,125	70,58824	75	60,86957
2.9-0-2.9-0	62,5000	92,10526	83,33333	20	66,66667	90	23,68421	75	50	60,86957
0-2.9-0-2.9	100,0000	92,10526	100	45	80	90	37,5	96	48	70
0-2.9-0-2.9 q'=1-2-3-3	62,5000	50	100	39,13043	100	78,94737	100	96	40	93,33333
0-0-0-0 q'=1-2-3-3	62,5000	51,47059	100	39,13043	100	81,81818	90	100	46,15385	100

M3x	M3y	M3z	M3	<M3	M4x	M4y	M4z	M4	<M4	
83,33333	80	100	90	88,88889	38,46154	40	97,5	57,14286	86,95652	1340,5805
83,33333	63,15789	87,5	90	88,88889	38,46154	94,11765	97,5	66,66667	80	1540,6866
89,28571	61,53846	93,333333	100	100	35,71429	84,21053	97,5	57,14286	80	1533,8004
83,33333	80	89,74359	94,736842	61,53846	100	45,71429	100	66,66667	80	1474,2384
83,33333	80	87,5	91,836735	80	29,41176	57,14286	86,666667	66,66667	80	1353,4022
83,33333	72,72727	89,74359	93,75	100	38,46154	53,33333	93,975904	100	76,92308	1521,1034
100	80	87,5	91,836735	100	25	80	97,5	66,66667	80	1451,3923
83,33333	63,15789	89,74359	100	66,66667	21,73913	57,14286	97,5	66,66667	66,66667	1453,0792
86,2069	63,15789	87,5	91,836735	100	27,77778	57,14286	91,764706	66,66667	80	1404,8813
100	80	89,74359	100	100	45,45455	94,11765	97,5	57,14286	83,33333	1491,5949
90,90909	70,58824	87,5	93,75	100	41,66667	100	97,5	66,66667	100	1472,7397
100	68,57143	93,333333	100	66,66667	20,83333	64	97,5	57,14286	100	1526,6529
71,42857	100	70	85,714286	44,44444	20	35,55556	78	57,14286	80	1402,1969
73,52941	96	89,74359	78,26087	47,05882	20	37,2093	78	57,14286	57,14286	1405,1608

6. Conclusion

The results shown in the paper, the researched active moments in some different cases of the robot's joints movements, the applied method, the proper algorithm, multi objective function (*MOF*) and the proper LabVIEW *VI*-s can be used in many other research in the robotics field.

Acknowledgment

The authors tanks for technical support to be possible this assisted research to University Politehnica of Bucharest, department of Robots and Production Systems, Industrial Engineering and Robotics Faculty, ACTTM Company from Bucharest, Centre for test- evaluation and scientific research for armaments, Techno Accord Mechatronics Company from Leuval, Quebec, Canada and Kosice University of Technology from Slovakia.

References

[1] Barral, D. & Perrin. J-P. & Dombre, E. & Lie'geois, A. (1999). Development of optimization tools in the context of an industrial robotic CAD software product, *International Journal of Advvanced Manufacturing Technology,* Vol. 15(11), pp. 822–831, doi: 10.1007/ s001700050138.

[2] Box, G.E.P. & Hunter, W.G. & Hunter, J.S. (1978). *Statistics for experimenters: an introduction to design, data analysis and model building*, Wiley, New York.

[3] Box, M. J., (1965). A New Method of Constrained Optimization and a Comparison with Other Methods, *Computer Journal*, Vol 8, pp. 42-52.

[4] Fardanesh, B. & Rastegar, J. (1988). Minimum cycle time location of a task in the workspace of a robot arm, *Proceeding of the IEEE 23rd Conference on Decision and Control*, pp. 2280–2283.

[5] Feng, X. & Sander, S.T. & Ölvander, J. (2007). Cycle-based Robot Drive Train Optimization Utilizing SVD Analysis, *Proceedings of the ASME Design Automation Conference*, Las Vegas, September 4-7, 2007.

[6] Haug, E.J. (1992). *Intermediate dynamics*, Prentice-Hall, Englewood Cliffs, NJ.

[7] Kamrani, B. & Berbyuk, V. & Wäppling, D. & Stickelmann, U. & Feng, X. (2009). Optimal Robot Placement Using Response Surface Method, *International Journal of Advvanced Manufacturing Technology*, Vol. 44, pp. 201-210.

[8] Khuri, A.I. & Cornell, J.A. (1987). *Response surfaces design and analyses*, Dekker, New York.

[9] Krus, P. & Jansson, A. & Palmberg, J-O. (1992). Optimization Based on Simulation for Design of Fluid Power Systems, *Proceedings of ASME Winter Annual Meeting*, Anaheim, USA 26 Robot Manipulators, Trends and Development.

[10] Luenberger, D.G. (1969). *Optimization by vector space methods*, Wiley, New York.

[11] Myers, R.H. & Montgomery, D. (1995). *Response surface methodology: process and product optimization using designed experiments*, Wiley, New York.

[12] Nelson, B. & Donath, M. (1990). Optimizing the location of assembly tasks in a manipulator's workspace, *Journal of Robotic Systems*, Vol 7(6), pp. 791–811, doi:10.1002/rob.4620070602.

[13] Pettersson, M. & Ölvander, J. (2009). Drive Train Optimization for Industrial Robots, *IEEE Transactions on Robotics*, to be published.

[14] Pettersson, M. (2008). *A PhD Dissertation*, Linköping University, Linköping, Sweden.

[15] Tsai, L.W. (1999). *Robot analysis*, Wiley, New York.

[16] Tsai, M.J. (1986). *Workspace geometric characterization and manipulability of industrial robot. Ph.D. Thesis,* Department of Mechanical Engineering, Ohio State University.

[17] Vukobratovic, M. (2002). Beginning of robotics as a separate discipline of technical sciences and some fundamental results—a personal view, *Robotica,* Vol. 20(2), pp. 223–235.

[18] Yoshikawa, T.(1985). Manipulability and redundancy control of robotic mechanisms, *Proceeding of the IEEE Conference on Robotics and Automation*, pp 1004–1009.

[19] Ölvander J. (2001). *Multiobjective Optimization in Engineering Design – Applications to Fluid Power Systems, A PhD Dissertation*, No. 675 at Linköping University.

[20] Smarandache Fl. *Neutrosophic theory*- Mc.Gallup- New Mexico

[21] Y. Chunyan & C.Wen, *Extenics Theory, Method and Applications*, Sciences Press, Beijing, 2013, ISBN 978-7-03-035989-6.

[22] Othayoth RS, Chittawadigi RG, Joshi RP, Saha SK. *Robot kinematics made easy using RoboAnalyzer software.* Comput Appl Eng Educ. 2017;9999:1–12. https://doi.org/10.1002/ cae.21828.

[23] F. A. Candelas, S.T. Puente, F. Torres, F. G. Ortiz, P. Gil, J. Pomares, *A virtual laboratory for teaching robotics,* Int J. Eng. Educ., 19 (2003), 363–370.

[24] C. A. Jara, F. A. Candelas, J. Pomares, F. Torres, *Java software platform for the development for advanced robotic virtual laboratories,* Comput. Appl. Eng. Educ., 21 (2013), 14–30.

[25] Navaraja,N.Jain,D.Sengupta,C.S.Kumar, Web based simulation and remote triggered laboratory for robots, *28th International Conference on CAD/CAM, Robotics and Factories of the Future*, 2016, 665–677.

[26] H. D. Nayar, Robotect: serial-link manipulator design software for modeling, visualization and performance analysis, *7th Int. Conf. Control, Autom., Robot. and Vision*, 2002, 1360–1364.

[27] M. Freese, S. Singh, F. Ozaki, N. Matsuhira, Virtual robot experimentation platform V-REP: a versatile 3D robot simulator, *Int. Conf. Simulation, Modeling, and Programming for Autonomous Robots*. 2010, 51–62.

[28] RoKiSim − available at: *http://www.parallemic.org/RoKiSim. html*. Accessed in June 2016.

[29] O. Michel, *Webots: professional mobile robot simulation*, Int J. Adv. Robot. Syst., 1 (2004), 39–42.

[30] A.Gil,O.Reinoso, J.M.Marin, L.Paya, J.Ruiz, *Development and deployment of a new robotics toolbox for education,* Comput. Appl. Eng. Educ., 23 (2015), 443–454. https://doi.org/10.1002/cae.21615.

[31] M.Flanders,R.Kavanaugh, Build-A-*Robot:using virtual reality to visualize the Denavit– Hartenberg parameters*, Comput. Appl. Eng. Educ., 23 (2015), 846–853.

[32] S. Kucuk, Z. Bingul, *An off-line robot simulation toolbox*, Comput. Appl. Eng. Educ.,18 (2010), 41–52.

[33] M. A. Gonzalez-Palacios, Advanced engineering platform for industrial development, *J. Appl. Res. Tech.*, 10 (2012), 309–326.

[34] M.A.Gonzalez-Palacios,E.A.Gonzalez-Barbosa,L.A.Aguilera- Cortes, *SnAM: a simulation software on serial manipulators,* Eng. Comput., 29 (2013), 87–94.

[35] M. Quigley, K. Conley, B. Gerkey, J. Faust, T. Foote, J. Leibs, E. Berger, R. Wheeler, A. Ng, ROS: an open-source robot operating system. *In ICRA Workshop on Open Source Software*, Vol. 3, No. 3.2, 2009.

[36] ROS – Gazebo Plugin, available at: *http://wiki.ros.org/gazebo*. Accessed on June 2016.

[37] Eulalie Coevoet, Thor Morales-Bieze, Frederick Largilliere, Zhongkai Zhang, Maxime Thieffry, et al.. *Software toolkit for modeling, simulation and control of soft robots. Advanced Robotics*, Taylor & Francis, 2017, pp.1-26. hal-01649355.

[38] Workspacelt. [Online]. Available: *http://www.workspacelt.com.*

[39] Roboticsimulation. [Online]. Available: *https://robologix.com.*

[40] Ni-robotics. [Online]. Available: *http://www.ni.com.*

[41] Robonaut. [Online]. Available: *http://robonaut.jsc.nasa.gov.*

[42] Simrobot. [Online]. Available: *http://www.informatik.uni-bremen.de.*

[43] Open dynamics engine. [Online]. Available: *http://ode.org.*

[44] Bullet physics. [Online]. Available: *http://bulletphysics.org.*

[45] Nvidia physx. [Online]. Available: *https://developer.nvidia.com/physx-sdk.*

[46] Dart. [Online]. Available: *http://dartsim.github.io*.

[47] Olaru, A., and S. Olaru. Assisted research of the industrial robot Fourier spectrum with LabVIEW instrumentation. *Annals of DAAAM & Proceedings*, 2005, p. 277+. *Gale Academic Onefile*, Accessed 4 Oct. 2019, Gale Document Number: GALE|A176688385.